Current Opinion in Solid State and Materials Science xxx (2016) xxx–xxx

Contents lists available at ScienceDirect

Current Opinion in Solid State and Materials Science

journal homepage: www.elsevier.com/locate/cossms

# Shape memory strains and temperatures in the extreme

H. Sehitoglu *, L. Patriarca [1], Y. Wu

*Department of Mechanical Science and Engineering, University of Illinois at Urbana-Champaign, 1206 W. Green Street, Urbana, IL 61801, USA*

ARTICLE INFO

*Article history:*
Received 5 January 2016
Revised 20 April 2016
Accepted 19 June 2016
Available online xxxx

*Keywords:*
Shape memory alloys
NiTiHf
Transformation strain
Transformation temperature
Slip resistance

ABSTRACT

It is well known that the achievement of high transformation strains in shape memory alloys (SMAs) has been curtailed by plastic deformation mediated via dislocation slip. In particular, the utilization of SMAs at high temperatures is also hindered by plastic slip. In this paper, an overview of the most important SMAs is provided by constructing transformation strain, transformation temperature, and slip resistance plots to put existing works in perspective. To this plots, we added results on NiTiHf alloys which impart both high temperature capability and high slip resistance at unprecedented levels. The remarkable finding is that NiTiHf alloys can undergo transformation strains near 20% and transformation temperatures exceeding 400 °C.

© 2016 Published by Elsevier Ltd.

## 1. Introduction

The SMAs have been the subject of intense scientific curiosity since their discovery more than 50 years ago. Several books have been written which have covered the state of art in the 1980s through the 2000s [1–5]. Many ongoing symposia on martensitic phase transformations, such as ICOMAT (International Conference on Martensitic Transformations) and ESOMAT (European Symposium on Martensitic Transformations), are now focused heavily on SMA centric research. A new journal exclusively on SMA, under the aegis of American Society of Metals International and Shape Memory and Superelastic Technologies (SMST), was launched last year [5]. The quest to reach higher transformation temperatures while not compromising slip resistance is ongoing, as evidenced from special symposia on the topic of high temperature SMAs (HTSMAs) and many recent works. There are also advantages in extending the transformation recoverability to high strains to improve fatigue and fracture resistance. Despite these intense activities in SMA research, the success in raising the transformation strain, transformation temperatures and slip resistance, beyond 12%, 250 °C and 1 GPa respectively, has remained elusive. In this paper we provide an overview of the current SMAs and discuss their high temperature, high strain capabilities and flow resistance, before presenting results on the NiTiHf system. We then outline conclusions and future directions.

It is instructive to define the unique behavior of SMAs with the aid of Fig. 1. The 'transformation strain', the 'slip resistance' and the 'transformation temperature' parameters are all marked in Fig. 1. The transformation strain can be obtained from three types of experiments: strain recovery upon heating (called shape memory effect (SME)), strain recovery upon unloading (called superelasticity (SE)), and the strain recoverability upon heating and cooling under isobaric conditions (ISME). The 'transformation strain' is marked for ISME case in the schematic in Fig. 1. The transformation strain results for all three cases should agree, in principle. At low temperatures, martensite twinning occurs and deformation is recovered upon heating (SME). The martensite 'twinning stress' is marked in Fig. 1. In the stress induced transformation region, the 'transformation stress' increases with increasing temperature and superelastic response (SE) is observed above the austenite finish temperature. The austenite finish temperature is designated as the 'transformation temperature' in Fig. 1. At high temperature, the 'slip stress of austenite' decreases with increasing temperature. The slip resistance corresponds to the critical stress level at the $M_d$ temperature. The $M_d$ temperature is the highest temperature above which martensite can no longer be stress-induced. Above $M_d$, the material flows via plastic deformation. The dislocation flow stress of austenite (above $A_f$) is important, because during the transformation processes the austenite slip at the A/M interfaces, and in adjacent matrix domains, can render the process irreversible at the micro-scale.

Early emphasis in SMAs focused on experimentation with copper based alloys [4,6] that show excellent transformation strains but poor plastic deformation resistance [7–9]. They are no longer pursued vigorously because of their weak fatigue response and dis-

* Corresponding author
*E-mail address:* huseyin@illinois.edu (H. Sehitoglu).
[1] Currently at Politecnico di Milano, Milano, Italy.

http://dx.doi.org/10.1016/j.cossms.2016.06.005
1359-0286/© 2016 Published by Elsevier Ltd.

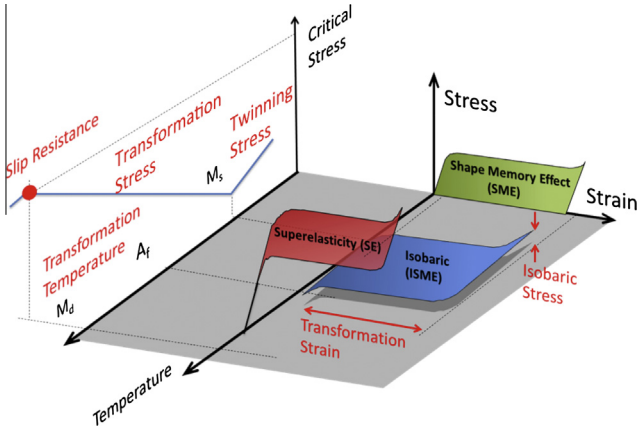


**Fig. 1.** The demonstration of the three key parameters in shape memory alloys that are highlighted in this study. The 'Slip Resistance' is defined as the flow stress of austenite, the 'Transformation Temperature' is defined as austenite finish temperature, and the 'Transformation Strain' is obtained from one of three type of experiments SME = Shape memory effect, SE = Superelasticity, and ISME = Isobaric Shape Memory Effect.

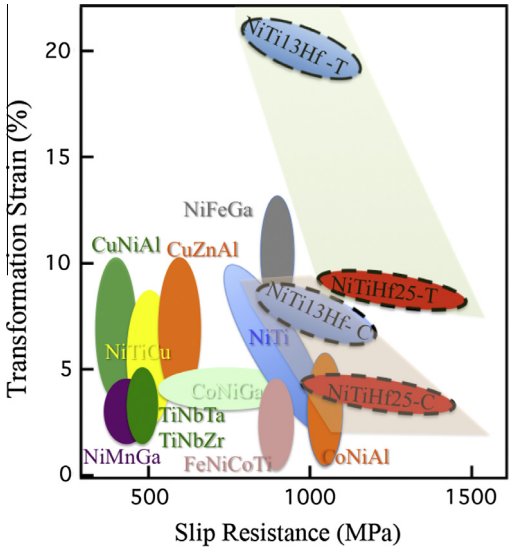


**Fig. 2.** Transformation strain–slip resistance plot showing the most well-known SMAs in comparison with the NiTiHf alloys. The tension results are separated from the compression results by shading with a different color.

location slip-induced irreversibility [7,8,10,11]. The discovery of NiTi with its remarkable properties has revolutionized the SMA research field [12]. Not only does the NiTi exhibit good transformation strains, it has excellent plastic slip resistance imparting stable response over many cycles [13,14]. The NiTi alloys have a maximum transformation strain of 10% and this has been viewed as a ceiling [15,16]. There are advantages in developing SMAs that give higher transformation strains because this will result in higher damage tolerance and better functional properties for applications. We also note that the use of NiTi is limited to less than 75 °C [17]. At elevated temperatures, the activation of slip and diffusional effects impedes the reversibility of transformation [18]. The development of higher temperature SMAs (HTSMAs) continues to remain challenging. Ideally, higher transformation temperatures (near 400 °C) could open significant applications in various industries. In this regard, the NiTiHf alloys permit high maximum strain, high transformation temperature and possess excellent slip resistance and is the topic of this paper.

### 1.1. Transformation strain-slip resistance behavior of SMAs

In Fig. 2, we provide a combined transformation strain – slip resistance plot. The most important observation that stands out in Fig. 2 is the ultra-high strains for the case of NiTiHf (~50.3 at.% Ni, 13.3 at.% or 25 at.% Hf, Ti balance, designated as $NiTiHf_{13.3}$ and $NiTiHf_{25}$ respectively) in tension which we expound in the next section. We assert that the slip resistance of the B2 NiTiHf alloys exceeds other SMA materials. For $NiTiHf_{13.3}$ and $NiTiHf_{25}$, we indicate the tension and compression levels (tension versus compression denoted by –T versus –C respectively), as well as the potential range of slip resistance associated with thermo-mechanical treatments. The difference in tension and compression is primarily attributed to the transformation planes having low symmetry indices, i.e. the habit plane system [19]. The difference between $NiTiHf_{13.3}$and $NiTiHf_{25}$ transformation strains is the increased volume fraction of precipitates and the increased presence of the orthorhombic martensite domains with increasing Hf contents.

Most ordered SMAs, such as B2, exhibit strong plastic flow resistance [20]; the disordered alloys, such as fcc or bcc crystal structures, have weaker slip resistance but can be strengthened via precipitation hardening (upon aging) or ordering treatments [21–24]. The precipitates can be used to tailor transformation temperatures [25], reduce hysteresis [26,27], adjust the transformation stress [17] which are all beneficial. They do reduce the transformation strains to a smaller degree [28], the benefits outweigh the decrease in transformation strains. The transformation strain also depends on the composition of the alloys. Even small changes in the alloy content in NiTi are known to have dramatic effect on the results. This sensitivity to composition exists with other alloys as well. As stated above, the strain levels in most SMAs are below 10%. The alloys that have been of considerable focus in early works include the Cu based SMAs with seemingly excellent functionality suffer from poor plastic deformation resistance. The $Ni_2FeGa$ and CoNiAl(Ga) alloys stand out as potentially very good candidates as they exhibit both favorable strains and slip resistance [29–31]. Their transformation strains are in the range 6–12% for cubic to tetragonal transformation. Their transformation behavior is highly orientation dependent and they need heavy texturing which precludes their widespread application. The NiMnGa alloys are brittle in tension and they can only be used in compression; nonetheless they have potential utility as ferro-magnetic shape memory alloys. Other SMAs, such as Fe-based alloys have better plastic deformation resistance but limited transformation strains (<4%). The FeNiCoAlTi needs fine precipitates for slip resistance in an fcc matrix. It exhibits limited strains and large hysteresis and no superelastic behavior. The new FeMnAlNi based alloys (not shown in the figure) with bcc to fcc transformation exhibit surprising superelasticity [32], but low plastic flow resistance [33]. The Ti-Ta and Ti-Nb alloys exhibit moderate transformation strains (6% max.) and good plastic slip resistance depending on the ternary additions [34]. Further work is needed in Ti based SMAs before their potential utilization.

The transformation strain is also influenced by the propensity of some SMAs to show incomplete phase transformation which inhibits the achievement of the theoretical values. We draw a distinction between local strain measurements utilizing high resolution digital image correlation and the overall strain measurements using extensometry. In NiTiHf alloys, we emphasize that the local strain measurements are needed to gain an understanding of the intrinsic transformation strains because of spatial non uniformity of strains. In other SMAs, such as in high Ni (51.5%Ni) NiTi the strain fields were also nonuniform [28] with maximum value of 4% while in ≪51%Ni NiTi alloys the local and overall strains are

Please cite this article in press as: H. Sehitoglu et al., Shape memory strains and temperatures in the extreme, Curr. Opin. Solid State Mater. Sci. (2016), http://dx.doi.org/10.1016/j.cossms.2016.06.005

found to be much closer [35] with maximum value of 10% in 50.1% Ni [28]. The spread of transformation strains (10–2%) in Figs. 2 and 3 for NiTi represent the results obtained from single crystals with compositions in the range 50.1–51.8%Ni respectively.

In the case of $Ni_2FeGa$ [36] and CuZnAl alloys (unpublished), our DIC results show that the transformation zone spreads to the entire gage section upon large deformations, so the local and overall strains are similar at 12 and 9% respectively. Similarly, the strains have been found to be uniform across the gage length in $Ni_2MnGa$ [37]. For $Ni_2MnGa$, the results plotted in Figs. 2 and 3 correspond to compression case because of the lack of ductility in tension. The transformation strain results in SMAs depend on the sample crystal orientation, therefore single crystals (or highly textured polycrystals) with maximum strain capability (intrinsic values) should be selected. These orientations are near [001] for $Ni_2FeGa$, CuZnAl, CoNiAl and near [111] in NiTi alloys for tension. The strain magnitudes given in Fig. 2 and 3 reflect these intrinsic, maximum strain values.

We note that the calculated martensite CRSS levels using DFT are rather high compared to austenite (for example 1.1 GPa versus 0.63 GPa for NiFeGa). This is true for most SMAs. The austenite slip stress levels for SMAs ($Ni_2FeGa$, $Co_2NiGa$, $Co_2NiAl$, NiTi, CuZn and $Ni_2TiHf$) which possess the $L1_2$ and B2 cubic structures were predicted with PN (Peierls-Nabarro) theory [20,38]. Interestingly, the critical stress for CuZn, is found to be 80 MPa. This alloy suffers from plastic deformation and exhibits the lowest levels. For austenitic NiTi the most likely slip system is $(011)[100]$ with a CRSS of 0.71 GPa consistent with experiments. The theoretical calculations for CRSS in $Ni_2FeGa$, $Co_2NiGa$, $Co_2NiA$, NiTi, $NiTiHf_{25}$, and CuZn results in 0.63, 0.76, 0.72, 0.71, 0.78 and 0.08 GPa respectively [38]. These values are consistent with corresponding experimental values presented in [20,39–47].

### 1.2. Transformation strain-transformation temperature behavior of SMAs

The transformation temperatures at 400 °C and above makes NiTiHf alloys attractive candidates for high temperature SMA applications. We show examples of $NiTiHf_{13.3}$ and $NiTiHf_{25}$ results in Fig. 3. Previous works explored the transformation temperatures with change in Hf contents in the range 15–20 at.% [48–50]. Transformation temperatures less than 250 °C have been reported depending on the Ni/Hf content. The transformation temperatures for alloys with Ni content lower than 50% exhibit higher values compared to Ni-rich compositions but do not show superelasticity. Most recently, the use of 25 at.% Hf NiTiHf in nickel-rich polycrystals [51] resulted in higher transformation temperatures. Therefore, further presentation of experimental data on these alloys is of considerable interest.

As stated earlier, the transformation temperatures in SMAs with good functional properties are typically less than 100 °C for most cases (Fig. 3). The most well-known NiTi alloys are utilized below 75 °C. Although the $Ni_2FeGa$ and CoNiGa (Al) alloys can exhibit superelasticity at temperatures above 75 °C [30,31], their austenite finish temperature is less than 50 °C. Therefore, they cannot be used as an actuator at high temperatures. The CuZnAl, CuNiAl, and FeNiCoTi alloys are limited to temperatures less than 100 °C [2,10,11,22,52–55]. The NiMnGa which exhibits useful SMA behavior at temperatures less than 100° is utilized in the martensitic state [56,57]. Recent introduction of Nb, Ta, and Zr ternary elements [34,58] in TiTa and TiNb alloys have opened new possibilities. The transformation temperatures of these alloys can approach 300 °C, but the transformation strains have been limited. The TiPd [59,60] and TiAu [61,62] alloys can reach higher transformation temperatures but have not been well studied, so they are not discussed in this paper. In perspective, they can benefit from further research to improve their mechanical properties.

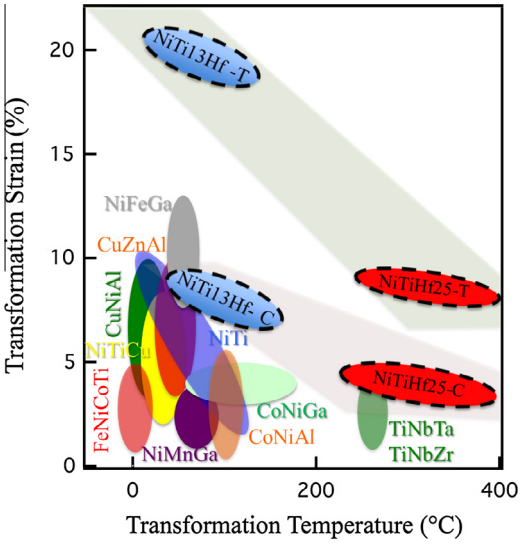


**Fig. 3.** Transformation strain–transformation temperature plot showing the most well-known SMAs in comparison with the NiTiHf alloys.

## 2. New insights into NiTiHf alloys- towards superior SMAs

### 2.1. Overview of previous NiTiHf work

We provided an overview of the entire shape memory arena summarizing the most pertinent metrics in Figs. 2 and 3. Early work on NiTiHf alloys has given insight on the physical metallurgy and metallurgical processing studies [63–65]. Few preliminary studies on the mechanical behavior of different Hf contents were made from early 2000, in particular focusing on the shape memory response of bent plates [66–68]. Because of elastic recovery and tension-compression symmetry it is difficult to interpret bending results. Shape memory behavior of bent samples displayed transformation strains up to 6.25% for the $Ni_{49}Ti_{36}Hf_{15}$ composition [69,70], even though the low Ni content of this alloy (<50%) precludes its usage as superelastic material. In the last years the interest on the mechanical behavior of NiTiHf is growing, and several studies have shown good SME, ISME and SE behaviors at temperatures above 250 °C. Transformation strains up to 3.74% in polycrystal were obtained for the $Ni_{50.3}Ti_{29.7}Hf_{20}$ composition [71–75]. Remarkably, superelastic behavior was found at temperatures as high as 240 °C [73]. In view of the promising results for the polycrystal, single crystals of $Ni_{50.3}Ti_{29.7}Hf_{20}$ alloy showed only comparable level of transformation strains. The $Ni_{50.3}Ti_{29.7}Hf_{20}$ [111] orientation was tested in isobaric compression experiments, and transformation strains up to 3.9% were measured [72]. However, further efforts in testing different crystal orientations ([001], [340], [678], [011]) did not lead to higher transformation strains. In our previous work, we selected a higher Hf content (25 at.%) in order to explore transformation temperatures higher than 250 °C. In compression, we obtained local transformation strains of 3.25% at temperatures higher than 265 °C [76]. Even though the strain measurements refer to small domains in the polycrystalline material, the results show that, potentially, along specific crystal orientations the $NiTiHf_{25}$ can promote concurrently high transformation strains and high transformation temperatures. Moreover, the Ni content can be properly manipulated in the compositional range of 50–51 at.% in order to adjust transformations strains, temperatures and ductility. Regarding the slip resistance measure-

Please cite this article in press as: H. Sehitoglu et al., Shape memory strains and temperatures in the extreme, Curr. Opin. Solid State Mater. Sci. (2016), http://dx.doi.org/10.1016/j.cossms.2016.06.005

ments in the literature, one needs to conduct deformation experiments near the $M_d$ temperature to precisely pinpoint its value. Such measurements were reported to be near 1000 MPa for compositions of 20 and 12.5Hf [44,77]. The results for the 25Hf alloys in our work also correspond to slip stress near 1000 MPa. We note that as the Hf increases the $M_d$ temperature shifts to higher value which makes these alloys even more attractive as possessing strength at high temperatures.

Now, we want to detail the new results on NiTiHf alloys which hold considerable promise. Specifically, the emphasis will be placed on plastic deformation resistance, transformation strains and transformation temperatures, three major considerations that govern the SMA response. As discussed above, the NiTiHf alloys have the potential to exhibit ultra-high strains and also possess high operational temperatures. We highlight these attributes with several figures given below.

### 2.2. Experimental results on NiTiHf

In Figs. 4 and 5, the results display the SE+SME and the SE behavior for the $NiTiHf_{13.3}$ case for tension and compression, respectively. The experimental techniques are provided in Appendix A. In $NiTiHf_{13.3}$, the phase transformation is a consequence of cubic to monoclinic crystal lattice change under stress. Theoretically, the lattice constants and the monoclinic angle for NiTiHf favor high transformation strains. The first experiment in tension is conducted at 40 °C which is slightly below the austenite finish temperature. The material undergoes a combined SE+SME behavior. The superelastic response (2.5%) occurs upon unloading and the remnant strain (15%) is recovered at zero stress upon heating to a critical temperature. This recovery at zero stress is termed the shape memory effect (SME). The total recoverable strain levels are near 18%. We note that such a high transformation strain level can open new applications. Other experiments on the same alloy were conducted at higher temperatures (50 °C) with pure SE response and at low temperatures (−35 °C) with pure SME response [78]. The recoverable strains are in agreement with the values presented in Fig. 4. In compression (Fig. 5), we note that the SE response at room temperature with a recoverable strain exceeding 7% corresponds to stress levels of 1500 MPa. To our knowledge, SE at such high stresses combined with high strains (>7%) is unprecedented for NiTi based alloys. In binary NiTi alloys, the compressive strains are limited to less than 5.5%.

In Figs. 6 and 7, the results for isobaric temperature cycling (ISME) are provided for the $NiTiHf_{25}$ alloy for tension and compression, respectively. These experiments are begun by heating the alloy to high temperature and then applying a constant stress. During cooling and heating the stress is maintained constant. The images of the entire specimen surface are captured and stored for later analysis. The strain measurements at high magnifications represent the true transformation strains because the domains that are undergoing elastic deformation are excluded. We note that the strain distribution is more heterogeneous in tension compared to compression. The results show higher transformation strains in tension compared to compression with both values that are very high considering that the temperatures are near 450 °C. The results are shown for a cooling and heating cycle. Since both the transformation temperatures and the slip stresses in this alloy are high, these figures show excellent potential of $NiTiHf_{25}$. The strains reported in Figs. 6 and 7 are near 9% and 7% in tension and compression, respectively. In Fig. 6, at the martensite start temperature, the strains increase in the tensile direction. Because elastic energy opposes the transformation, further undercooling is needed to continue the transformation as evident from the slope of the strain-temperature curves [26]. Upon heating, the specimen reverts to austenite beginning at austenite start temperatures with

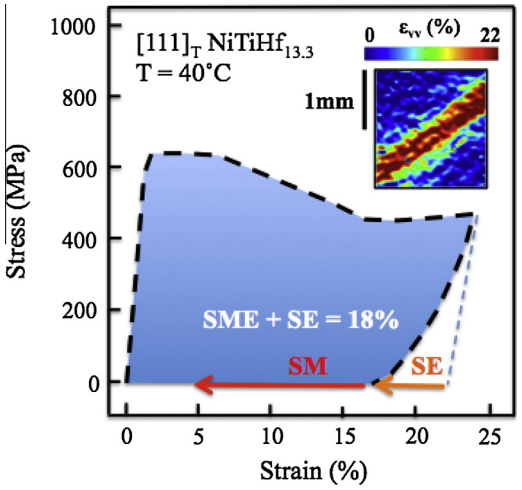


**Fig. 4.** The stress-strain response of NiTi13Hf demonstrating recoverable strains near 18% which is remarkably high (based on [78]).

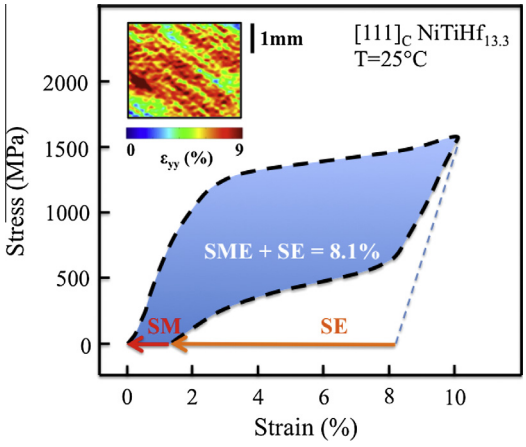


**Fig. 5.** The stress-strain response of NiTi13Hf demonstrating strains above 8% with stress levels near 1500 MPa (see also [78]).

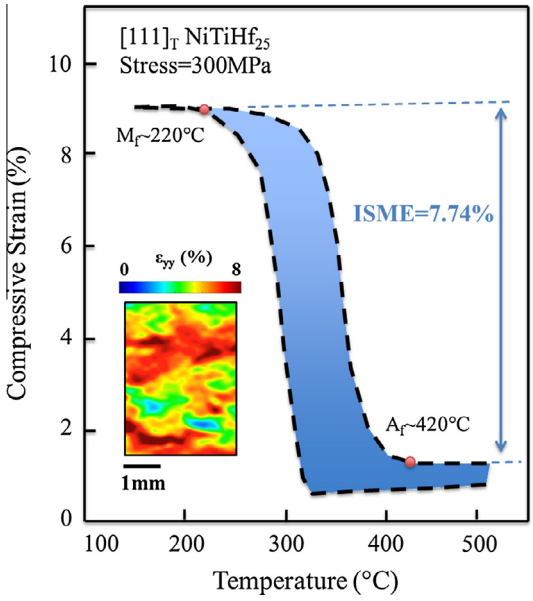


**Fig. 6.** The strain-temperature response of $NiTiHf_{25}$ demonstrating strains exceeding 7.7% with austenite finish temperature of 420° (from reference [79]).

Please cite this article in press as: H. Sehitoglu et al., Shape memory strains and temperatures in the extreme, Curr. Opin. Solid State Mater. Sci. (2016), http://dx.doi.org/10.1016/j.cossms.2016.06.005

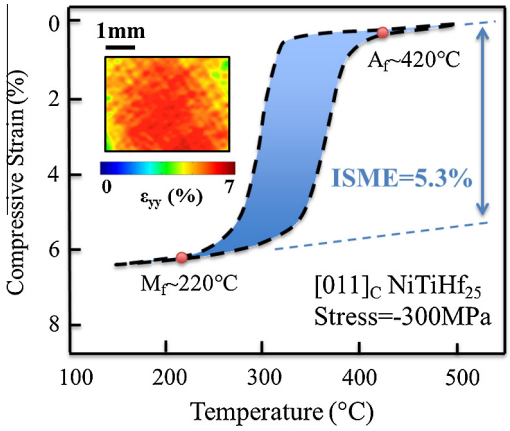


**Fig. 7.** The strain-temperature response of $NiTiHf_{25}$ demonstrating strains of 6% with austenite finish temperature of 420° (based on [79]).

the transformation completing at the austenite finish temperature. It is important to note that the thermal hysteresis associated with the transformation remains below 60 °C despite the high operating temperatures. This data is obtained from reference [79].

## 3. Discussion of results

The search and discovery of new materials that far exceed the capabilities of the present ones must remain a tenet of research enterprise. This is particularly true for the shape memory alloy field because once can achieve significantly different behaviors in transformation strains, transformation temperatures with small changes in composition. The field evolved from Cu alloys to NiTi based alloys to encompass materials with exceedingly high strains, high temperatures and excellent resistance to plastic deformation. One must continue to seek compositions that favorably change the lattice constants hence result in large transformation strains. At the same time the alloys must possess considerable plastic deformation resistance to withstand such high strains in a thermoelastic deformation. The high transformation temperature SMA NiTiHf alloys fulfill these functionalities.

A natural question that arises is why the NiTiHf exhibits such high strengthening levels compared to other ternary additions. Among these ternary elements, Hf has the largest atomic radius exceeding the values for Pt, Pd, Cu and Fe. The presence of Hf changes the bond lengths between Ni and Ti atoms within the lattice elevating the fault energy curves, hence the slip stresses [80]. Another factor is the presence of precipitates that impart slip resistance. The structure of precipitate has been reported by Santamarta et al. [30]. Essentially, the precipitate structure observed in the present alloys has been published earlier [77]. Fig. 8 (a) and (b) indicates that there are three sets of B19′ martensite plate consisting of $(0\,0\,1)_{B19'}$ compound twins marked as A, B and C. There are also 1/3 $110*_{B2}$ type reflections derived from precipitate marked as P in Fig. 8(b). Further studies are needed on the role of precipitates on the transformation stress and hysteresis in view of their well-known influence in binary alloys.

The other question has to do with the reasons behind the large transformation strains in NiTiHf alloys [81]. The lattice constants for austenite and martensite and the monoclinic angle of the martensite dictate the stretch tensors. Especially, the monocolinic angle increase can be substantial with increasing Hf content (from 96.8° to 105.9° for 25Hf). Further work is needed for enhanced understanding in this area. We note that one reason why the transformation strains are saturating as the Hf content is increased is due to the presence of increasing volume fraction of precipitates constituting domains which cannot undergo transformation.

The results of this study shows that $NiTiHf_{13.3}$ and $NiTiHf_{25}$ exhibit ductilities as high as 22% and 10% in tension, respectively. These tensile ductilities exceed the fracture strains of many of the SMAs that are summarized in Figs. 2 and 3. As discussed in early works [82], void nucleation and void coalescence at the matrix/precipitate interfaces are precursors to fracture. Therefore, the solutionized microstructural states may offer advantages in addition to texturing to have favorable orientations that circumvent the activation of {001} and {110} cleavage planes.

As previously discussed, the recent body of work on NiTiHf alloys [50,72,75,83] has considered both polycrystals and single crystals for Hf contents less than 20 at.%. These recent works on compression have shown that the transformation strains fall far below the theoretical values [75]. A similar discrepancy has been observed in NiTi alloys in early work [27]. However, the reported difference between theory and experiment in NiTiHf alloys is far more severe. The present results overcome this seeming anomaly by making local DIC measurements and noting that there are substantial untransformed domains for both the 13.3Hf and 25Hf ternary compositions. Therefore, the overall measurements with extensometry may not be representative of the intrinsic transformation strains in SMAs with a heterogeneous microstructure.

The results underscore the advantages of studying a lower Hf content near 13 at.% Hf to provide a better assessment of transformation strain change with increasing Hf content. The 13Hf alloy present higher slip resistance compared to other ternary additions and demonstrate very high strains. At the local level, the strains can exceed 20% in experiments which points to possible role of reversible mechanical twinning contributing to additional strains. Unlike other SMAs the mechanical twinning is possibly reversible in the case NiTiHf alloys with high slip resistance. Theoretical calculations of twinning stress confirm its operation well below the slip stress [80]. Further work is needed to explain the origin of such high reversible strains.

Other measures of SMA performance can be studied but are viewed as application specific. For example, the work output of shape memory alloys can be an important consideration in actuators. The work output is defined as stress times the transformation strain in an ISME experiment. Work outputs exceeding 20 J/m$^2$ are considered to be exceptional. Another parameter is the thermal/stress hysteresis which is an important quantity in an actuator and in damping respectively. Thermal hysteresis is the width of the strain-temperature curves in an ISME experiment [26]. In NiTi the range is between 40 and 80° [26] which is similar in NiTiHf alloys (50 °C on the average as shown in Figs. 6 and 7). The R-Phase in NiTi is considered to have tiny hysteresis, albeit with small transformation strains, and has found niche applications. The NiFeGa alloys exhibit exceptionally low thermal hysteresis [31]. There are ongoing explorations of alternative ferromagnetic shape memory alloys (Fe and Co based) [84] to NiMnGa to achieve functionality in tension and improve ductility. For superior ferromagnetic shape memory, the elastic strain energy needs to be low while the magnetic anisotropy energy has to be high to overcome the elastic strain energy. So far, the NiMnGa remains the best ferromagnetic shape memory alloy. The cost of the SMAs is another important metric. The addition of Pd, Pt, Au to binary NiTi has been considered but these ternary elements are very expensive. The Hf is also an expensive element and worthy of specialized high temperature applications. Other alloys such as $Ni_2MnGa$, $Ni_2FeGa$ are also costly because of the presence of gallium. The Cu and Fe based SMAs are less costly compared to the nickel and titanium based alloys. More details regarding the cost analysis are left aside for future papers. Finally, the entropy change associated with transformation can be an important consideration to maximize thermo-

Please cite this article in press as: H. Sehitoglu et al., Shape memory strains and temperatures in the extreme, Curr. Opin. Solid State Mater. Sci. (2016), http://dx.doi.org/10.1016/j.cossms.2016.06.005

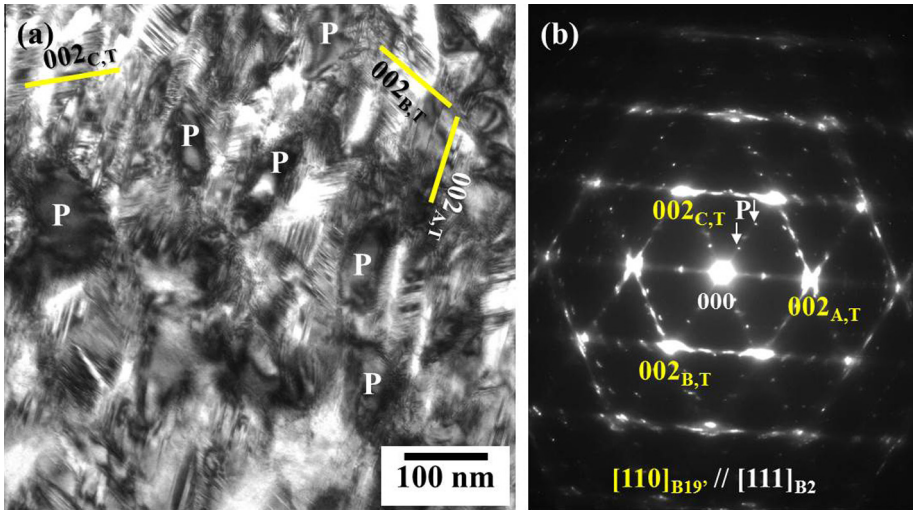


**Fig. 8.** (a) Bright field image and (b) corresponding electron diffraction pattern. The pattern shows three sets of $(0\,0\,1)_{B19'}$ compound twin and $1/3\ 110^*_{B2}$ type from precipitate (P) (from [77]).

elastocaloric effects [35], ie. cooling magnitudes. The entropy change correlates with the slope of the transformation stress-temperature curve which is unusually high for $NiTiHf_{13.3}$ alloy opening new possibilities [77]. Among SMAs the NiTi alloys possess some of the largest entropy changes [85]. These other considerations are left aside for future research reviews.

## 4. Conclusions and future directions

An overview of the shape memory field is given summarizing the capabilities of the current shape memory alloys. The work supports the following:

(1) Three key parameters that govern SMA functionality were identified. They are transformation strain, transformation temperature and plastic slip resistance. We provide a summary of the most important SMAs highlighting these three parameters.
(2) The current SMAs have served the community well with transformation strain levels near 10% and transformation temperature levels less than 75 °C. The slip resistance ($\ll$1000 MPa) has limited the widespread utilization of a number of SMAs where fatigue and fracture resistance is of paramount importance.
(3) The present results underscore the need for high transformation temperatures (>400 °C) and high transformation strains (>20%). We used a mutiscale approach to measure the transformation strains in NiTiHf alloys precisely, demonstrating superlative functionalities. The results are convincing and repeatable. Our results and experiments (SME, SE and ISME behaviors) notwithstanding, we point to the need for study of new class of SMAs.
(4) Further work is needed to optimize the compositions and heat treatments as the NiTi alloys with ternary additions such as NiTiHf are rather complex in their response and in their underlying microstructure.

## Acknowledgements

The work is supported by a National Science Foundation grant NSF CMMI-1333884 which is gratefully acknowledged. The single crystals of NiTiHf were grown by Prof. Yuriy Chumlyakov. The authors of the paper thank the reviewers for their valuable comments.

## Appendix A

### A.1. Experimental techniques

The NiTiHf single crystals reported in this study were grown by the Bridgman technique in He atmosphere. The rods were sectioned into disks parallel to the (0 1 1) crystallographic plane using electrical discharge machining. For the $NiTiHf_{25}$ composition the tensile specimens were successively cut along the [1 1 1] orientation, while the compression specimens along the [0 1 1] orientation. For the $NiTiHf_{13.3}$ composition both the tensile and compression specimens were cut along the [1 1 1] orientation. The characterization of the microstructure can be found in Ref. [77]. The tensile specimens were shaped into dog-bone geometry with 3 mm × 1.5 mm net section and 10 mm gauge length, while the compression specimens were sectioned into 4 mm × 4 mm × 9 mm geometry.

### A.2. Digital image correlation

The strain measurements are made with advanced digital image correlation (DIC) methods. In DIC, images of the deformed region of interest are correlated to a reference image (of the same region prior to deformation) to make full-field measurements of displacements. The in-plane strain fields are calculated, afterwards, through differentiation of the vertical and horizontal displacement fields [86]. The resolution of the strain field depends on the magnification at which reference and deformed images are captured [87]. For the experiments presented in this work, the compression and tension specimens were initially polished with abrasive paper up to 1800 grit. The speckle pattern for DIC strain measurements was deposited using an Iwata Micron B airbrush and a black paint for high temperature applications. The images were successively captured with a resolution ranging between 2 μm/px and 3 μm/px. The DIC contour plots in Figs. 4–7 always display the axial component (parallel to the load direction) of the strain tensor. By considering single crystals and using digital image correlation it is possible to make measurements without the grain boundary effects that can produce superfluous strain gradients.

Please cite this article in press as: H. Sehitoglu et al., Shape memory strains and temperatures in the extreme, Curr. Opin. Solid State Mater. Sci. (2016), http://dx.doi.org/10.1016/j.cossms.2016.06.005

Prior to loading, the orientations of the specimens were verified with X-ray diffraction performed on a Philips Xpert 2 diffractometer using Cu Kα radiation. For the $NiTiHf_{25}$ alloy, the X-ray diffraction orientation data were acquired at 500 °C in the fully austenitic phase.

### A.3. Tension and compression experiments

The tension and compression experiments were conducted on a servo-hydraulic machine under quasi-static conditions. The load frame was controlled with a customized Labview program. For both tension and compression isothermal experiments the loading was conducted under displacement control and unloading was performed under stress control providing an average strain rate of $10^{-3}$ $s^{-1}$. The specimen surface images were obtained synchronously with the load data and stored for later analysis. During isothermal deformation the images were captured every 2 s. The temperature of the specimens was measured using a Epsilon laser based measurement system. The specimens were heated with a Lepel 2.5 kW Induction Heater. Specimen cooling was obtained in air for the high temperature $NiTiHf_{25}$ alloy, while we used liquid nitrogen in order to cool the grips for the experiments on the $NiTiHf_{13.3}$ alloy.

During isobaric experiments one initial reference image was captured at the maximum temperature and at zero stress. At the maximum temperature the constant stress was successively applied and a second image captured. Successively, the images for DIC were manually captured every 5 °C. To input the NiTiHf results into Figs. 2 and 3 we conducted in excess of 75 experiments in total.

## References

[1] K. Otsuka, C.M. Wayman, Shape Memory Materials, Cambridge University Press, Cambridge, 1998.
[2] T.W. Duerig KNM, K.N. Melton, D. Stöckel, C.M. Wayman (Eds.), Engineering Aspects of Shape Memory Alloys, Butterworth-Heinemann, Boston, 1990.
[3] H. Funakubo, Shape Memory Alloys, Gordon and Breach Science Publishers, 1987 (translated from the Japanese by J.B. Kennedy).
[4] J. Perkins, Shape Memory Effects in Alloys, Springer US Publisher, 1975.
[5] H. Sehitoglu, A new journal helping to shape the future of materials, Shape Mem. Superelast. 1 (2015) 1–3.
[6] L. Delaey, R.V. Krishnan, H. Tas, H. Warlimont, Thermoelasticity, pseudoelasticity and the memory effects associated with martensitic transformations, J. Mater. Sci. 9 (1974) 1521–1535.
[7] C. Damiani, F.C. Lovey, M. Sade, Plastic deformation under compression of Cu–Zn–Al martensitic single crystals, Mater. Sci. Eng. A (Struct. Mater.: Prop. Microstruct. Process.) A323 (2002) 436–444.
[8] M. Sade, E. Hornbogen, Fatigue of single- and polycrystalline -CuZn-base shape memory alloys, Zeitschrift fur Metallkunde 79 (1988) 782–787.
[9] L. Delaey, J. Janssen, D. Van de Mosselaer, G. Dullenkopf, A. Deruyttere, Fatigue properties of pseudoelastic Cu–Zn–Al alloys, Scr. Metall. 12 (1978) 373–376.
[10] L.C. Brown, The fatigue of pseudoelastic single crystals of-CuAlNi, Metall. Trans. A (Phys. Metall. Mater. Sci.) 104 (1979) 217–224.
[11] K.N. Melton, O. Mercier, Fatigue of NiTi and CuZnAl shape memory alloys, in: Strength of Metals and Alloys 5th International Conference, 27–31 Aug 1979, Pergamon, New York, NY, USA, 1979, pp. 1243–1248.
[12] W.J. Buehler, J.V. Gilfrich, R.C. Wiley, Effect of low-temperature phase changes on the mechanical properties of alloys near composition TiNi, J. Appl. Phys. 34 (1963) 1475–1477.
[13] K. Gall, H.J. Maier, Cyclic deformation mechanisms in precipitated NiTi shape memory alloys, Acta Mater. 50 (2002) 4643–4657.
[14] B. Strnadel, S. Ohashi, H. Ohtsuka, S. Miyazaki, T. Ishihara, Effect of mechanical cycling on the pseudoelasticity characteristics of Ti–Ni and Ti–Ni–Cu alloys, Mater. Sci. Eng., A 203 (1995) 187–196.
[15] S. Miyazaki, S. Kimura, F. Takei, T. Miura, K. Otsuka, Y. Suzuki, Shape memory effect and pseudoelasticity in a Ti-Ni single crystal, Scr. Metall. 17 (1983) 1057–1062.
[16] S. Miyazaki, K. Otsuka, Y. Suzuki, Transformation pseudoelasticity and deformation behavior in a Ti–50.6 at%Ni alloy, Scr. Metall. 15 (1981) 287–292.
[17] H. Sehitoglu, I. Karaman, R. Anderson, X. Zhang, K. Gall, H. Maier, Y. Chumlyakov, Compressive response of NiTi single crystals, Acta Mater. 48 (2000) 3311–3326.
[18] J. Ma, I. Karaman, R.D. Noebe, High temperature shape memory alloys, Int. Mater. Rev. 55 (2010) 257–315.
[19] K. Gall, H. Sehitoglu, The role of texture in tension-compression asymmetry in polycrystalline NiTi, Int. J. Plast. 15 (1999) 69.
[20] T. Ezaz, J. Wang, H. Sehitoglu, H.J. Maier, Plastic deformation of NiTi shape memory alloys, Acta Mater. 61 (2013) 67–78.
[21] H. Sehitoglu, C. Efstathiou, H.J. Maier, Y. Chumlyakov, Hysteresis and deformation mechanisms of transforming FeNiCoTi, Mech. Mater. 38 (2006) 538.
[22] H. Sehitoglu, X.Y. Zhang, T. Kotil, D. Canadinc, Y. Chumlyakov, H.J. Maier, Shape memory behavior of FeNiCoTi single and polycrystals, Metall. Mater. Trans. A (Phys. Metall. Mater. Sci.) 33A (2002) 3661.
[23] Y.I. Chumlyakov, I.V. Kireeva, O.A. Kutz, A.S. Turabi, H.E. Karaca, I. Karaman, Unusual reversible twinning modes and giant superelastic strains in FeNiCoAlNb single crystals, Scripta Mater. 119 (2016) 43–46.
[24] L.W. Tseng, J. Ma, I. Karaman, S.J. Wang, Y.I. Chumlyakov, Superelastic response of the FeNiCoAlTi single crystals under tension and compression, Scripta Mater. 101 (2015) 1–4.
[25] A.J. Wagoner Johnson, R.F. Hamilton, H. Sehitoglu, G. Biallas, H.J. Maier, Y.I. Chumlyakov, H.S. Woo, Analysis of multistep transformations in single-crystal NiTi, Metall. Mater. Trans. A (Phys. Metall. Mater. Sci.) 36A (2005) 919–928.
[26] R.F. Hamilton, H. Sehitoglu, Y. Chumlyakov, H.J. Maier, Stress dependence of the hysteresis in single crystal NiTi alloys, Acta Mater. 52 (2004) 3383.
[27] H. Sehitoglu, R. Hamilton, D. Canadinc, X.Y. Zhang, K. Gall, I. Karaman, Y. Chumlyakov, H.J. Maier, Detwinning in NiTi alloys, Metall. Mater. Trans. A 34 (2003) 5–13.
[28] C. Efstathiou, H. Sehitoglu, Local transformation strain measurements in precipitated NiTi single crystals, Scripta Mater. 59 (2008) 1263.
[29] Y.I. Chumlyakov, I.V. Kireeva, E.Y. Panchenko, E.E. Timofeeva, Z.V. Pobedennaya, S.V. Chusov, I. Karaman, H. Maier, E. Cesari, V.A. Kirillov, High-temperature superelasticity in CoNiGa, CoNiAl, NiFeGa, and TiNi monocrystals, Russ. Phys. J. 51 (2008) 1016–1036.
[30] R.F. Hamilton, H. Sehitoglu, C. Efstathiou, H.J. Maier, Y. Chumlyakov, Pseudoelasticity in Co–Ni–Al single and polycrystals, Acta Mater. 54 (2006) 587.
[31] R.F. Hamilton, H. Sehitoglu, C. Efstathiou, H.J. Maier, Inter-martensitic transitions in Ni–Fe–Ga single crystals, Acta Mater. 55 (2007) 4867–4876.
[32] Y. Tanaka, Y. Himuro, R. Kainuma, Y. Sutou, T. Omori, K. Ishida, Ferrous polycrystalline shape-memory alloy showing huge superelasticity, Science 327 (2010) 1488–1490.
[33] L.W. Tseng, J. Ma, S.J. Wang, I. Karaman, M. Kaya, Z.P. Luo, Y.I. Chumlyakov, Superelastic response of a single crystalline FeMnAlNi shape memory alloy under tension and compression, Acta Mater. 89 (2015) 374–383.
[34] P.J.S. Buenconsejo, H.Y. Kim, H. Hosoda, S. Miyazaki, Shape memory behavior of Ti–Ta and its potential as a high-temperature shape memory alloy, Acta Mater. 57 (2009) 1068–1077.
[35] G.J. Pataky, E. Ertekin, H. Sehitoglu, Elastocaloric cooling potential of NiTi, Ni2FeGa, and CoNiAl, Acta Mater. 96 (2015) 420–427.
[36] C. Efstathiou, H. Sehitoglu, J. Carroll, J. Lambros, H.J. Maier, Full-field strain evolution during intermartensitic transformations in single-crystal NiFeGa, Acta Mater. 56 (2008) 3791–3799.
[37] R. Hamilton, S. Dilibal, H. Sehitoglu, H. Maier, Underlying mechanism of dual hysteresis in NiMnGa single crystals, Mater. Sci. Eng., A 528 (2011) 1877–1881.
[38] J. Wang, H. Sehitoglu, H.J. Maier, Dislocation slip stress prediction in shape memory alloys, Int. J. Plast. 54 (2014) 247–266.
[39] Y. Chumlyakov, I. Kireeva, E. Panchenko, E. Timofeeva, Z. Pobedennaya, S. Chusov, I. Karaman, H. Maier, E. Cesari, V. Kirillov, High-temperature superelasticity in CoNiGa, CoNiAl, NiFeGa, and TiNi monocrystals, Russ. Phys. J. 51 (2008) 1016–1036.
[40] I. Karaman, D.C. Lagoudas, Magnetic Shape Memory Alloys with High Actuation Forces, DTIC Document, 2006.
[41] S. Dilibal, H. Sehitoglu, R. Hamilton, H. Maier, Y. Chumlyakov, On the volume change in Co–Ni–Al during pseudoelasticity, Mater. Sci. Eng., A 528 (2011) 2875–2881.
[42] C. Efstathiou, H. Sehitoglu, Local transformation strain measurements in precipitated NiTi single crystals, Scripta Mater. 59 (2008) 1263–1266.
[43] H. Sehitoglu, J. Jun, X. Zhang, I. Karaman, Y. Chumlyakov, H.J. Maier, K. Gall, Shape memory and pseudoelastic behavior of 51.5%Ni–Ti single crystals in solutionized and overaged state, Acta Mater. 49 (2001) 3609–3620.
[44] D. Coughlin, P. Phillips, G. Bigelow, A. Garg, R. Noebe, M. Mills, Characterization of the microstructure and mechanical properties of a 50.3 Ni–29.7 Ti–20 Hf shape memory alloy, Scripta Mater. 67 (1) (2012) 112–115.
[45] Y. Wang, Y. Zheng, W. Cai, L. Zhao, The tensile behavior of Ti36Ni49Hf15 high temperature shape memory alloy, Scripta Mater. 40 (1999) 1327–1331.
[46] R. Romero, F. Lovey, M. Ahlers, Plasticity in Œ⩽ phase Cu–Zn–Al alloys, Philos. Mag. A 58 (1988) 881–903.
[47] J.A. Wollmershauser, S. Kabra, S.R. Agnew, In situ neutron diffraction study of the plastic deformation mechanisms of B2 ordered intermetallic alloys: NiAl, CuZn, and CeAg, Acta Mater. 57 (2009) 213–223.
[48] H. Karaca, S. Saghaian, B. Basaran, G. Bigelow, R. Noebe, Y. Chumlyakov, Compressive response of nickel-rich NiTiHf high-temperature shape memory single crystals along the [111] orientation, Scripta Mater. 65 (2011) 577–580.
[49] A.P. Stebner, G.S. Bigelow, Y. Jin, D.P. Shukla, S.M. Saghaian, R. Rogers, A. Garg, H.E. Karaca, Y. Chumlyakov, K. Bhattacharya, R.D. Noebe, Transformation strains and temperatures of a nickel-titanium-hafnium high temperature shape memory alloy, Acta Mater. 76 (2014) 40–53.

Please cite this article in press as: H. Sehitoglu et al., Shape memory strains and temperatures in the extreme, Curr. Opin. Solid State Mater. Sci. (2016), http://dx.doi.org/10.1016/j.cossms.2016.06.005

[50] A. Evirgen, I. Karaman, R. Santamarta, J. Pons, R.D. Noebe, Microstructural characterization and shape memory characteristics of the Ni50.3Ti34.7Hf15 shape memory alloy, Acta Mater. 83 (2015) 48–60.
[51] L. Patriarca, H. Sehitoglu, High-temperature superelasticity of Ni 50.6 Ti 24.4 Hf 25.0 shape memory alloy, Scripta Mater. 101 (2015) 12–15.
[52] R. Stalmans, J. Van Humbeeck, L. Delaey, Degradation of the shape memory effect in copper-base alloys, Scr. Metall. Mater. 31 (1994) 1573–1576.
[53] R. Stalmans, J. van Humbeeck, L. Delaey, Thermomechanical cycling, two way memory and concomitant effects in Cu–Zn–Al alloys, Acta Metall. Mater. 40 (1992) 501–511.
[54] C.M. Friend, L. Manosa, J. Ortin, A. Planes, A calorimetric investigation of martensitic transformation under applied stress in single crystal Cu–Al–Ni alloys, in: European Symposium on Martensitic Transformation and Shape Memory Properties, 16–18 Sept 1991. France, C4 ed., 1991, pp. 71–76.
[55] J. Van Humbeeck, D. Van Hulle, L. Delaey, J. Ortin, C. Segui, V. Torra, A two-stage martensite transformation in a Cu–13.99 mass% Al–3.5 mass% Ni alloy, Trans. Jpn. Inst. Met. 28 (1987) 383–391.
[56] P.J. Webster, K.R.A. Ziebeck, S.L. Town, M.S. Peak, Magnetic order and phase transformation in Ni2MnGa, Philos. Mag. Part B 49 (1984) 295–310.
[57] A. Sozinov, A.A. Likhachev, N. Lanska, K. Ullakko, Giant magnetic-field-induced strain in NiMnGa seven-layered martensitic phase, Appl. Phys. Lett. 80 (2002) 1746–1748.
[58] S. Miyazaki, H.Y. Kim, H. Hosoda, Development and characterization of Ni-free Ti-base shape memory and superelastic alloys, Mater. Sci. Eng., A 438 (2006) 18–24.
[59] M. Nishida, T. Hara, Y. Morizono, A. Ikeya, H. Kijima, A. Chiba, Transmission electron microscopy of twins in martensite in Ti-Pd shape memory alloy, Acta Mater. 45 (1997) 4847–4853.
[60] R. Arockiakumar, M. Takahashi, S. Takahashi, Y. Yamabe-Mitarai, Microstructure, mechanical and shape memory properties of Ti–55Pd–5x (x=Zr, Hf, V, Nb) alloys, Mater. Sci. Eng., A 585 (2013) 86–93.
[61] C. Declairieux, A. Denquin, P. Ochin, R. Portier, P. Vermaut, On the potential of Ti50Au50 compound as a high temperature shape memory alloy, Intermetallics 19 (2011) 1461–1465.
[62] P. Vermaut, C. Declairieux, P. Ochin, V. Kolomytsev, A. Pasko, G. Monastyrsky, A. Denquin, R. Portier, Martensitic transformation and shape memory effect at very high temperatures in HfPd, and TiAu intermetallic compounds, J. Alloy. Compd. 577 (2013) 388–392.
[63] P. Potapov, A. Shelyakov, A. Gulyaev, E. Svistunov, N. Matveeva, D. Hodgson, Effect of Hf on the structure of Ni–Ti martensitic alloys, Mater. Lett. 32 (1997) 247–250.
[64] S. Besseghini, E. Villa, A. Tuissi, Ni–Ti–Hf shape memory alloy: effect of aging and thermal cycling, Mater. Sci. Eng., A 273–275 (1999) 390–394.
[65] P.E. Thoma, J.J. Boehm, Effect of composition on the amount of second phase and transformation temperatures of NixTi90−xHf10 shape memory alloys, Mater. Sci. Eng., A 273–275 (1999) 385–389.
[66] Y.Q. Wang, Y.F. Zheng, W. Cai, L.C. Zhao, The tensile behavior of Ti36Ni49Hf15 high temperature shape memory alloy, Scripta Mater. 40 (1999) 1327–1331.
[67] B. Kockar, I. Karaman, J.I. Kim, Y. Chumlyakov, A method to enhance cyclic reversibility of NiTiHf high temperature shape memory alloys, Scripta Mater. 54 (2006) 2203–2208.
[68] X.L. Meng, W. Cai, Y.D. Fu, Q.F. Li, J.X. Zhang, L.C. Zhao, Shape-memory behaviors in an aged Ni-rich TiNiHf high temperature shape-memory alloy, Intermetallics 16 (2008) 698–705.
[69] M.M. Javadi, M. Belbasi, M.T. Salehi, M.R. Afshar, Effect of aging on the microstructure and shape memory effect of a hot-rolled NiTiHf alloy, J. Mater. Eng. Perform. 20 (2011) 618–622.
[70] M. Moshref-Javadi, S.H. Seyedein, M.T. Salehi, M.R. Aboutalebi, Age-induced multi-stage transformation in a Ni-rich NiTiHf alloy, Acta Mater. 61 (2013) 2583–2594.
[71] G.S. Bigelow, A. Garg, S.A. Padula Ii, D.J. Gaydosh, R.D. Noebe, Load-biased shape-memory and superelastic properties of a precipitation strengthened high-temperature Ni 50.3Ti 29.7Hf 20 alloy, Scripta Mater. 64 (2011) 725–728.
[72] H.E. Karaca, S.M. Saghaian, B. Basaran, G.S. Bigelow, R.D. Noebe, Y.I. Chumlyakov, Compressive response of nickel-rich NiTiHf high-temperature shape memory single crystals along the [111] orientation, Scripta Mater. 65 (2011) 577–580.
[73] H.E. Karaca, S.M. Saghaian, G. Ded, H. Tobe, B. Basaran, H.J. Maier, R.D. Noebe, Y.I. Chumlyakov, Effects of nanoprecipitation on the shape memory and material properties of an Ni-rich NiTiHf high temperature shape memory alloy, Acta Mater. 61 (2013) 7422–7431.
[74] O. Benafan, A. Garg, R.D. Noebe, G.S. Bigelow, S.A. Padula Ii, D.J. Gaydosh, N. Schell, J.H. Mabe, R. Vaidyanathan, Mechanical and functional behavior of a Ni-rich Ni50.3Ti 29.7Hf20 high temperature shape memory alloy, Intermetallics 50 (2014) 94–107.
[75] A.P. Stebner, G.S. Bigelow, J. Yang, D.P. Shukla, S.M. Saghaian, R. Rogers, A. Garg, H.E. Karaca, Y. Chumlyakov, K. Bhattacharya, R.D. Noebe, Transformation strains and temperatures of a nickel–titanium–hafnium high temperature shape memory alloy, Acta Mater. 76 (2014) 40–53.
[76] L. Patriarca, H. Sehitoglu, High-temperature superelasticity of Ni50.6Ti24.4Hf25.0 shape memory alloy, Scripta Mater. 101 (2015) 12–15.
[77] Y. Wu, L. Patriarca, G. Li, H. Sehitoglu, Y. Soejima, T. Ito, M. Nishida, Shape memory response of polycrystalline NiTi12.5Hf alloy: transformation at small scales, Shap Mem. Superelast. 1 (2015) 387–397.
[78] Y. Wu, L. Patriarca, H. Sehitoglu, Y. Chumlyakov, Ultrahigh tensile transformation strains in new Ni50.5Ti36.2Hf13.3 shape memory alloy, Scripta Mater. 118 (2016) 51–54.
[79] L. Patriarca, Y. Wu, H. Sehitoglu, Y.I. Chumlyakov, High temperature shape memory behavior of Ni50.3Ti25Hf24.7 single crystals, Scripta Mater. 115 (2016) 133–136.
[80] J. Wang, H. Sehitoglu, Modelling of martensite slip and twinning in NiTiHf shape memory alloys, Philos. Mag. 94 (2014) 2297–2317.
[81] Y. Wu, A. Ojha, L. Patriarca, H. Sehitoglu, Fatigue crack growth fundamentals in shape memory alloys, Shap Mem. Superelast. 1 (2015) 18–40.
[82] Y. Chumlyakov, S. Efimenko, I. Kireeva, E. Panchenko, H. Sehitogly, K. Gall, H. Yahia, Effects of shape memory and superelasticity in aged TiNi single crystals, Dokl. Phys. 46 (2001) 849–852.
[83] S.M. Saghaian, H.E. Karaca, H. Tobe, M. Souri, R. Noebe, Y.I. Chumlyakov, Effects of aging on the shape memory behavior of Ni-rich Ni50.3Ti29.7Hf20 single crystals, Acta Mater. 87 (2015) 128–141.
[84] J. Pons, E. Cesari, C. Seguí, F. Masdeu, R. Santamarta, Ferromagnetic shape memory alloys: alternatives to Ni–Mn–Ga, Mater. Sci. Eng., A 481–482 (2008) 57–65.
[85] K. Niitsu, Y. Kimura, X. Xu, R. Kainuma, Composition dependences of entropy change and transformation temperatures in Ni-rich Ti–Ni system, Shap Mem. Superelast. 1 (2015) 124–131.
[86] M.A. Sutton, W.J. Wolters, W.H. Peters, W.F. Ranson, S.R. McNeill, Determination of displacements using an improved digital correlation method, Image Vis. Comput. 1 (1983) 133–139.
[87] C. Efstathiou, H. Sehitoglu, J. Lambros, Multiscale strain measurements of plastically deforming polycrystalline titanium: role of deformation heterogeneities, Int. J. Plast. 26 (2010) 93.

Please cite this article in press as: H. Sehitoglu et al., Shape memory strains and temperatures in the extreme, Curr. Opin. Solid State Mater. Sci. (2016), http://dx.doi.org/10.1016/j.cossms.2016.06.005